

Investigation of Structure and Morphology Dynamics in Tin Fluorophosphate Glass – Polyethylene Hybrids Using Solid-State ^1H , ^{13}C , and ^{31}P MAS NMR

Brad C. Tischendorf,[†] Douglas J. Harris,[‡] Joshua U. Otaigbe,[†] and Todd M. Alam^{*,‡}

Department of Material Science and Engineering, Iowa State University, Ames, Iowa 50011,
and Department of Organic Materials, Sandia National Laboratories,
Albuquerque, New Mexico 87185-0888

Received July 16, 2001. Revised Manuscript Received October 26, 2001

The variations in morphology and local structure in a series of tin fluorophosphate glass–polyethylene (TFPPE) hybrids were investigated using solid-state ^1H , ^{13}C , and ^{31}P MAS NMR. The combination of direct polarization ^{13}C MAS NMR experiments with various delay times and carbon spin–lattice relaxation filtered cross-polarized MAS NMR experiments allowed quantification of the monoclinic, orthorhombic, amorphous, and intermediate phases in the low-density polyethylene (LDPE) component of the TFPPE hybrids. These ^{13}C MAS NMR results showed an increase in the crystallinity with the addition of tin fluorophosphate (TFP) glass into the hybrids. The ^{31}P MAS NMR spectra reveal major changes in the local structure of the TFP glass component, with several new phosphorus species being formed during the production of the hybrid. The results of the ^1H – ^{13}C and ^1H – ^{31}P 2D wide line spectroscopy experiments demonstrate that all of these new phosphorus species are spatially correlated with the two new proton species that appear in the ^1H MAS NMR of the TFPPE hybrids. There is no evidence of correlation between these new phosphorus species and the methylene protons of the LDPE polymer component.

Introduction

Glass–polymer hybrids have the advantage of improved mechanical properties without increasing cost or the difficulty of processing.^{1–4} Traditionally E-glass or other types of silicate-based glass systems have been used to produce polymer–glass hybrids.⁴ These hybrids have the disadvantages of having to be processed with the glass in the solid state and are, in general, comparatively expensive. Because of these reasons, among others, there has been a recent increase in the use of phosphate glasses to produce melt-mixed hybrid materials.^{1,3–8} The two materials studied here were polyethylene and tin fluorophosphate glass. Polyethylene (PE) is used widely in a variety of different applications.^{9–14} Tin fluorophosphate (TFP) glasses on the other hand,

have limited applications, but recent reports demonstrate an increasing range of possibilities. Low-temperature water resistant SnF_2 – SnO – P_2O_5 glasses have been proposed for ophthalmic application.¹⁵ Similarly, Sn–Zn phosphate glasses have also been proposed as a lead-free alternative for the production of sealing frits.^{16,17} In addition, SnF_2 – SnO – P_2O_5 glass systems have been developed as host materials for organic chromophores for use in optical devices.^{18,19} It is the low glass transition temperature (T_g) of these TFP glasses (~ 120 °C) that make them prime candidates in the production of glass–polymer hybrids.

These hybrid materials have been shown to have both interesting morphologies and mechanical properties.^{1–3} Understanding the morphology and local structure of these glass–polymer hybrids is important in explaining the observed physical properties. In addition, this knowledge is required to tailor the microstructure and properties of the hybrids for specific applications. Solid-state NMR has become a versatile method for studying both polymer and glass systems.²⁰ There have been numerous solid-state NMR investigations of PE and

* To whom correspondence should be addressed. E-mail: tmalam@sandia.gov.

[†] Department of Material Science, Iowa State University.

[‡] Organic Materials Department, Sandia National Laboratories.

(1) Adalja, S. A. Masters Thesis, Iowa State University, 2000.
(2) Adalja, S. B.; Otaigbe, J. U. *Appl. Rheol.* **2001**, *11*, 10.
(3) Adalja, S. A.; Otaigbe, J. U.; Thalacker, J. *Polym. Eng. Sci.* **2001**, *41*, 1055.

(4) *MRS Bull.* **2001**, *26*, 364–408.

(5) Knowles, J. C.; Hastings, G. W. *J. Mater. Sci.: Mater. Med.* **1993**, *4*, 102.

(6) Otaigbe, J. U.; Beall, G. H. *Trends Polym. Sci.* **1997**, *5*, 369.
(7) Young, R. T.; Baird, D. G. *Annu. Technol. Conf. – Soc. Plast. Eng.* **1998**, *56th*, 2271.

(8) Young, R. T.; Baird, D. G. *Int. Polym. Process.* **2000**, *15*, 317.
(9) Krohn, J. V.; Todd, W. G.; Culter, J. D. *Polym., Laminations Coat. Conf.* **1998**, *1*, 397.

(10) Megremis, S. J.; Duray, S.; Gilbert, J. L. *ASTM Spec. Technol. Publ.* **1998**, *1346*, 235.

(11) Kozakiewicz, J.; Wielgosz, Z. *Pop. Plast. Packag.* **1999**, *44*, 53.
(12) Kartalis, C. N.; Papaspyrides, C. D.; Pfaendner, R. *Polym. Degrad. Stab.* **2000**, *70*, 189.

(13) Mikrajuddin; Shi, F. G.; Nieh, T. G.; Okuyama, K. *Microelectron. J.* **2000**, *31*, 261.

(14) Vulic, I.; Samuels, S. B.; Wagner, A. H.; Eng, J. M. *Pop. Plast. Packag.* **2000**, *45*, 68.

(15) Tick, P. A. *Phys. Chem. Glasses* **1984**, *25*, 149.

(16) Busio, M.; Steigelmann, O. *Glastech Ber. Glass Sci. Technol.* **2000**, *73*, 319.

(17) Morena, R. *J. Non-Cryst. Solids* **2000**, *263*–264, 382.

(18) Tick, P. A.; Hall, D. W. *Diff. Defect Data* **1987**, *53*–54, 179.

(19) Jiang, S.; Luo, T.; Wang, J.-F. *J. Non-Cryst. Solids* **2000**, *263*–264, 358.

(20) Schmidt-Rohr, K.; Spiess, H. W. *Multidimensional Solid-State NMR and Polymers*; Academic Press: New York, 1994.

other crystalline polymer systems, as well as several investigations of phosphate glass systems.^{21,22} Solid-state ¹³C NMR has been used to examine and quantify the crystalline, amorphous, and intermediate components in PE.^{23–28} Recent work by Hu and Schmidt-Rohr²³ have produced a new solid-state MAS NMR methodology for quantification of the different components using a combination of direct polarization (DP), cross-polarized (CP) MAS, and carbon spin-lattice relaxation time (T_{1C}) filtered CPMAS ¹³C NMR.²⁹ A wide variety of experimental techniques have been used to determine the structure of the tin fluorophosphate glass systems. These have included IR, Raman, XPS, Mossbauer spectroscopy, HPLC, and EXAFS.^{30–32} Until this time, there has been very limited NMR work done on TFP glass systems and no reported NMR work on phosphate glass/polymer hybrids.

In this investigation we report the ¹H, ¹³C, and ³¹P MAS NMR along with the ¹H-¹³C, and the ¹H-³¹P wide-line spectroscopy (WISE) results for a series of tin fluorophosphates-polyethylene (TFPPE) hybrids. Using these NMR results, changes in both the PE polymer morphology and the local TFP glass structure can be addressed. In addition, information about the interface between these two components is also discussed.

Experimental Procedures

Preparation of Hybrid Material. The glass used for these experiments was prepared from stoichiometrically calculated amounts of ammonium dihydrogen phosphate ($\text{NH}_4\text{H}_2\text{PO}_4$), tin oxide (SnO), and tin fluoride (SnF_2) to form the tin fluorophosphate (TFP) glass system with the nominal composition $50\text{SnF}_2\cdot20\text{SnO}\cdot30\text{P}_2\text{O}_5$. Ground and mixed batches of 30 g were placed in vitreous carbon crucibles and heated at 425 ± 10 °C for 25 min. Pouring them onto a cool steel plate quenched the samples to the vitreous state.^{31,32} The glass polymer hybrids were prepared from the $50\text{SnF}_2\cdot20\text{SnO}\cdot30\text{P}_2\text{O}_5$ base glass and low-density polyethylene (LDPE, PE 1035) obtained from Huntsman Chemical Corporation. All of the materials used were dried for at least 24 h at 100 °C under vacuum before use. A Brabender Measuring Head (C. W. Brabender Instruments, Inc.) torque mixer with twin roller-type rotors was used to prepare the hybrids. The mixer was preheated to 140 °C with a fixed shear rate of 30 rpm. The LDPE polymer was first added to the mixing head of the mixer and maintained at 140 °C for 5 min until a homogeneous melt was achieved. Subsequently, the

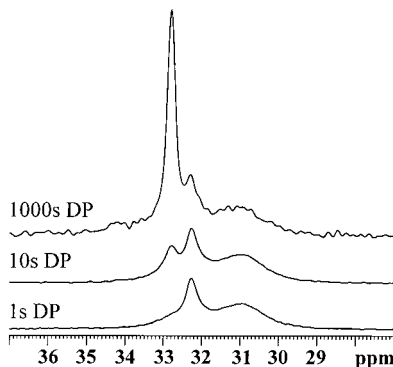


Figure 1. ¹³C MAS NMR spectra for the 10% TFPPE composite for a 1 s recycle delay, 10 s recycle delay and a 1000 s recycle delay. The variation of the relative prominence of the different phases within the polyethylene component of the polymer is visible.

glass was added as an unsized ball-milled powder and the mixture was melt-mixed for 20 min until completely homogeneous. A number of hybrids with TFP glass loading of 10%, 30%, and 50 vol % were prepared for this study. Additional details on the hybrid preparation method are available elsewhere.^{1–3}

DSC. The melting characteristics were investigated using a Perkin-Elmer Model DSC-7 after calibration with an indium standard. Samples with weights of approximately 10 mg were sealed in aluminum pans and analyzed with a scanning rate of 10 °C/min.

NMR Analyses. All solid-state MAS NMR experiments were performed on a Bruker AMX400 instrument operating at 100.6, 162.0, and 400.2 MHz for ¹³C, ³¹P, and ¹H, respectively. A 4-mm broadband MAS probe was used with sample spinning rates between 10 and 12.5 kHz. The different pulse sequences used in the analysis of the ¹³C MAS NMR experiments are shown in Figure 1S in the supporting material, with the methodology being detailed elsewhere.²³ All ¹³C pulse sequences employed a Hahn-echo to minimize baseline distortion, and utilized two pulse phase modulation (TPPM) ¹H decoupling.³³ One-dimensional (1D) DP MAS ¹³C spectra utilized long 1000 s recycle delays. DP spectra with shorter recycle delays (1 s and 10 s) required the modified sequence (Figure 1S) to remove nuclear Overhauser effects (NOE) by allowing the ¹H magnetization to fully relax. Both DP ¹³C experiments utilized a $3.8 \mu\text{s} \pi/2$ pulse, with 1–2K scans for the 10 s DP sequence and 24–48 scan averages for the 1000s DP sequence. The CPMAS experiments with and without a carbon spin-lattice relaxation time (T_{1C}) filter (Figures 1S) were obtained using a 0.5 ms contact time and a 5 s recycle delay. The T_{1C} filter experiments incorporate a delay during which the ¹³C magnetization undergoes spin-lattice decay prior to observation. All ¹³C chemical shifts were referenced to the crystalline PE peak ($\delta = +32.8$ ppm). The ³¹P MAS spectra were obtained with TPPM ¹H decoupling and utilized a single-pulse DP sequence with a $3.5 \mu\text{s} \pi/2$ pulse, a 60 s recycle delay and 512 scans, or a CPMAS sequence using a 2 ms contact time, a 4 s recycle delay, and 2K scans. The ³¹P chemical shifts were referenced externally to a secondary standard $(\text{NH}_4)\text{H}_2\text{PO}_4$ ($\delta = +0.8$

- (21) Brow, R. K. *J. Non-Cryst. Solids* **2000**, *263/264*, 1.
- (22) Kirkpatrick, R. J.; Brow, R. K. *Solid State Nucl. Magn. Reson.* **1995**, *5*, 9.
- (23) Hu, W.-G.; Schmidt-Rohr, K. *Polymer* **2000**, *41*, 2979.
- (24) VanderHart, D. L.; Khouri, F. *Polymer* **1984**, *25*, 1589.
- (25) Kuwabara, K.; Kaji, H.; Horii, F.; Bassett, D. C.; Olley, R. H. *Macromolecules* **1997**, *30*, 7516.
- (26) Eckman, R. R.; Henrichs, P. M.; Peacock, A. J. *Macromolecules* **1997**, *30*, 2474.
- (27) Cheng, J.; Fone, M.; Reddy, V. N.; Schwartz, K. B.; Fisher, H. B.; Wunderlich, B. *J. Polym. Sci., Polym. Phys. Ed.* **1994**, *22*, 589.
- (28) Kitamaru, R.; Horii, F.; Murayama, K. *Macromolecules* **1986**, *19*, 636.
- (29) Torchia, D. A. *J. Magn. Reson.* **1978**, *30*, 613.
- (30) Anma, M.; Yano, T.; Yasumori, A.; Hiroshi, K.; Yamane, M. *J. Non-Cryst. Solids* **1991**, *135*, 79.
- (31) Xu, X. J.; Day, D. E. *Phys. Chem. Glasses* **1990**, *31*, 183.
- (32) Brow, R. K.; Osborne, Z. A. *Surf. Interface Anal.* **1996**, *24*, 91.

- (33) Bennett, A. E.; Rienstra, C. M.; Auger, M.; Lakshmi, K. V.; Griffin, R. G. *J. Chem. Phys.* **1995**, *103*, 6951.

ppm with respect to 85% phosphoric acid $\delta = 0.0$ ppm). ^1H MAS spectra were obtained from single-pulse DP experiments on samples spinning at 10 kHz to obtain narrowed amorphous signals. All ^1H spectra were referenced to the main polyethylene resonance at $\delta = +1.3$ ppm. The two-dimensional (2D) ^1H - ^{13}C WISE experiments were obtained using a 1 ms CP contact time, 48 scan averages, 256 increments in the t_1 dimension, with a 250 kHz f_1 spectral width. The ^1H - ^{31}P 2D WISE experiments were obtained using a 2 ms CP contact time, 16 scan averages, 1024 increments in the t_1 direction, with a 250 kHz f_1 spectral width.

Results

A variety of NMR techniques were used to examine the TFPPE hybrids at three TFP glass compositions: 10%, 30%, and 50 vol %. Details of the changes in the PE phase morphology resulting from the addition of TFP glass and subsequent processing were examined using ^{13}C MAS NMR. Within the hybrid material, the TFP glass portion was studied using ^{31}P MAS NMR. In addition, a combination of ^{13}C , ^{31}P , and ^1H MAS along with ^1H - ^{31}P and ^1H - ^{13}C 2D WISE experiments were used to probe the interface between the polymer and phosphate glass within the hybrid material.

^{13}C MAS NMR. By evaluating the spectra obtained using a series of different ^{13}C pulse and recycle delays, the different phases within the polyethylene polymer can be identified and quantified. For example, at least four distinct phases are discernible in Figure 1 which shows the 1, 10, and 1000 s recycle delay DP MAS spectra for the 10 vol % TFPPE hybrid. In the 1 s DP spectrum (Figure 1, bottom), the fast relaxing amorphous phase is present as a broad peak centered at $\delta = +31.1$ ppm (Full Width Half Maximum (fwhm) ≈ 150 Hz). A second fast relaxing, nonpolyethylene resonance is also observed at $\delta = +32.3$ ppm (fwhm = 43 Hz). This resonance has been attributed to a bromine-containing flame retardant present within the starting polyethylene material. This assignment is consistent with the additional resonances observed at $\delta = +38.9$ and 60.3 ppm in both the solid state ^{13}C MAS NMR and the high-resolution solution ^{13}C NMR spectra of these materials (not shown). The intensity of this additive signal is $\sim 16\%$ of the total PE signal, and is constant for all of the materials investigated. In the 10 s DP spectra (Figure 1 middle) the broad, highly trans-chain intermediate polyethylene phase can be observed at $\delta = +32.9$ ppm (fwhm = 75 Hz). Finally, the crystalline orthorhombic $\delta = +32.8$ ppm (fwhm = 25 Hz) and monoclinic $\delta = +34.2$ ppm (fwhm = 40 Hz) phases appear for the 1000 s DP spectrum (Figure 1, top). These crystalline, intermediate, and amorphous phases clearly overlap, but differences in the relaxation properties allow them to be separated and quantified such that changes in the polyethylene morphology resulting from TFP glass addition can be determined (see discussion below).

The 1D ^{13}C CPMAS NMR spectra, using a 10 s $T_{1\text{C}}$ filter, are shown in Figure 2 for LDPE and the TFPPE hybrids investigated. Because of differences in the carbon spin–lattice relaxation times, the $T_{1\text{C}}$ filter sequence suppresses the rapidly relaxing amorphous and intermediate phase resonances, resulting in the

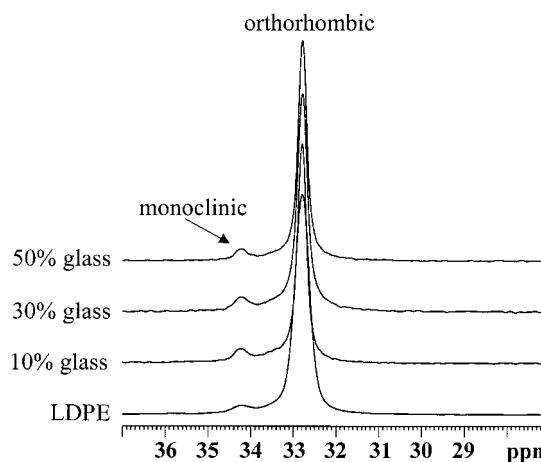


Figure 2. ^{13}C CPMAS NMR spectra using a 10 s $T_{1\text{C}}$ filter (Figure 1S in supporting material) for LDPE and the TFPPE composites. The $T_{1\text{C}}$ filter suppresses the signal from the amorphous and intermediate PE phases.

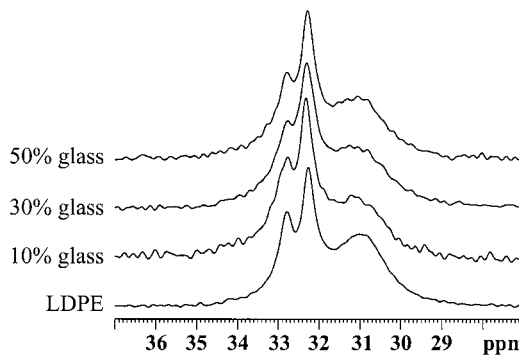


Figure 3. ^{13}C MAS NMR spectra with a 10 s recycle delay for LDPE and the TFPPE composites. This short recycle delay suppresses the signal from the carbons in the crystalline phases.

crystalline phases dominating the spectra in Figure 2. Both the monoclinic ($\delta = +34.2$ ppm) and orthorhombic ($\delta = +32.8$ ppm) crystalline phases are clearly visible within the LDPE and hybrids. The 10 s DP MAS spectra for LDPE and the TFPPE hybrids are shown in Figure 3, with the noncrystalline domains prominent in these spectra. No large differences in the crystalline or amorphous spectra are observed with increasing TFP glass concentration. A more quantitative analysis is therefore required.

Quantification of the four partially overlapping phases was obtained through line shape deconvolution, and difference spectroscopy, using a method recently described by Hu and Schmidt-Rohr.²³ Briefly, the amorphous polyethylene phase has a short ^{13}C spin–lattice relaxation time ($T_{1\text{C}} \approx 0.2$ s) and is almost completely relaxed after 1 s, while the interphase carbons have a slightly longer relaxation time but can be quantified from the 10 s DP spectra. The approximate line widths and chemical shifts of each component were determined from the 1 s DP MAS experiment and the difference between the 1 and 10 s DP experiments. For analysis of the crystalline phase, the 10 s ^{13}C DP MAS spectrum was subtracted from the 1000 s DP spectrum. The differential spectrum shows only the sharp orthorhombic and crystalline phases resulting from the long $T_{1\text{C}}$ relaxation times. The intensity of the isotropic crystalline signal was corrected for spinning sidebands ($\sim 3\%$

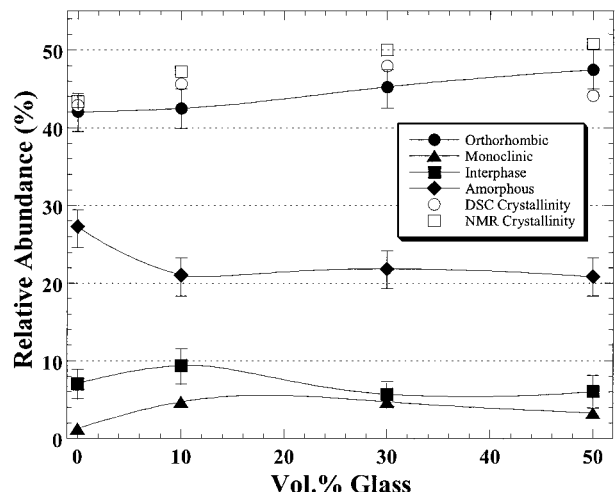


Figure 4. A plot of the relative fraction of the PE phases versus vol % fraction TFP glass in the TFPPE composites. Fractions were determined using ^{13}C MAS NMR (Table 1S in supporting material). The total crystallinity as determined from DSC analysis is also presented.

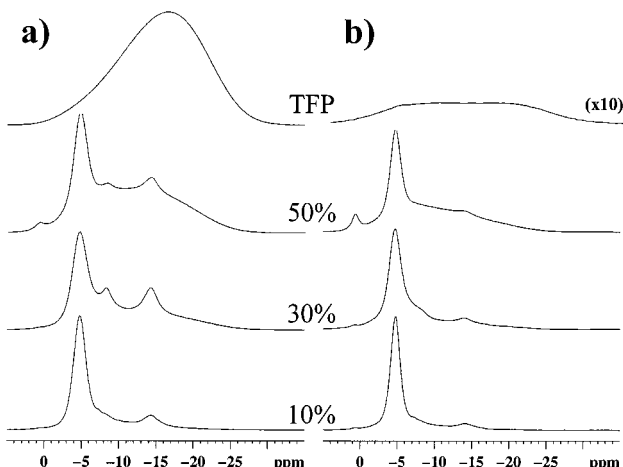


Figure 5. The isotropic chemical shift region of the ^{31}P MAS NMR spectra for the TFP glass and TFPPE composites using: a) direct polarization with a 60 s recycle delay, and b) CPMAS with a 2 ms contact time. Deconvolution results are detailed in Table 2S in supporting material.

at 10 kHz), and incomplete relaxation after 1000 s as determined by a 1000 s $T_{1\text{C}}$ -filtered CPMAS sequence. A correction for the crystalline relaxations during the short 10 s recycle delay was also included in the calculations. The relative fraction of the crystalline phases was finally determined from the corrected value of the crystalline integral compared with the integral of the ^{13}C DP MAS spectrum obtained with the 10 s recycle delay. For the TFPPE hybrids investigated, the variations in the relative fractions of these four phases with increasing TFP glass concentrations are shown in Figure 4. Additional details are given in Table 1S of the supporting material. Despite the complexity of this process, the NMR calculated crystallinity (the sum of the relative fraction of the orthorhombic and monoclinic phases) are in agreement with the DSC data (Figure 4 and Table 1S).

^{31}P MAS NMR. Direct polarization and CPMAS NMR spectrum for the TFPPE hybrids are shown in Figure 5. The isotropic spectral region of the hybrids reveals several overlapping resonances (the spectral

deconvolutions are summarized in Table 2S). For the as-prepared TFP glass only a single asymmetric broad resonance was observed at $\delta = -15.9$ ppm (fwhm = 2232 Hz). Inhomogeneously broadened ^{31}P MAS spectra are commonly observed in phosphate glasses, and reflect the large distribution in bond lengths and bond angles encountered in amorphous systems.³⁴ This asymmetric resonance was deconvoluted using two overlapping resonances at $\delta = -19.7$ ppm and $\delta = -13.5$ ppm. There have been no systematic NMR investigations of tin fluorophosphate glasses reported. There have been a few NMR studies of crystalline fluorophosphates,³⁵ along with fluorinated sodium phosphate and fluorinated sodium aluminophosphate glasses.³⁶ Brow and co-workers argue that if the fluorine is structurally incorporated in place of the bridging oxygen in the phosphate, the ^{31}P chemical shifts are very small because of the similarity of the electron density in the bridging P–O oxygen and the nonbridging P–F bonds.³⁶ Replacement of the nonbridging oxygen, however has a significant effect with the Q^1 pyrophosphate end group ($-\text{OP}(\text{O}^-)_3$) resonating at $\delta \sim -2$ ppm, while the fluorophosphate Q^1 species ($-\text{OP}(\text{O}^-)_2\text{F}$) is observed at $\delta = -17.9$ ppm (where the Q^n notation describes the different phosphate tetrahedral species, with $n = 0, 1, 2, 3$ representing the number of bridging oxygens attached to the phosphate). The ^{31}P chemical shifts of the Q^0 orthophosphate show a similar trend, with $(\text{P}(\text{O}^-)_4)$ being observed at $\delta = +11.7$ ppm and the monofluorophosphate $(\text{P}(\text{O}^-)_3\text{F})$ at $\delta = +5.7$ ppm.³⁶ In the pure TFP glass, the ^{31}P chemical shifts is consistent with the $(-\text{OP}(\text{O}^-)_2\text{F})$ fluorophosphate Q^1 species. The ^{31}P CPMAS spectra of the pure glass sample revealed weak overlapping resonances at $\delta = -18.7$ ppm and $\delta = -6.4$ ppm, which are different chemical shifts than that observed in the ^{31}P DP MAS spectrum. Based on the ^{31}P DP NMR spectra, these resonances that can be cross-polarized from ^1H comprise only 2 to 4% of the total ^{31}P signal. This weak CPMAS signal indicates that there is a low water concentration in the starting glass material, confirming our expectation of excellent durability of these particular glass systems. In addition, this limited CPMAS signal also demonstrates that the significant CP signal observed in the processed hybrids (see below) must result from ^1H introduced during the mixing with PE, and not from the original TFP glass.

With processing of the TFP glass into the hybrid, several changes are observed. As seen in Figure 5 (and Table 2S), the ^{31}P MAS spectra are now composed of several highly overlapping resonances. It is clear that there is a significant change in the glass structure during the preparation of the hybrid. There is a broad resonance (fwhm ~ 2400 Hz) at $\delta \sim -12$ ppm that steadily decreases in relative concentration with reduction of the TFP glass vol % fraction. This species may be closely related to the bulk glass resonance seen in the base TFP at $\delta = -13.5$ ppm since it is most prevalent at higher TFP glass concentrations, but the chemical shift is downfield shifted slightly and shows a ^1H CP signal. In the original TFP glass sample, the ^{31}P

(34) Alam, T. M.; Brow, R. K. *J. Non-Cryst. Solids* **1998**, 223, 1.

(35) Haubenreisser, U.; Sternberg, U.; Grimmer, A.-R. *Molecular Physics* **1987**, 60, 151.

(36) Brow, R. K.; Osborne, Z. A.; Kirkpatrick, R. J. *J. Mater. Res.* **1992**, 7, 1892.

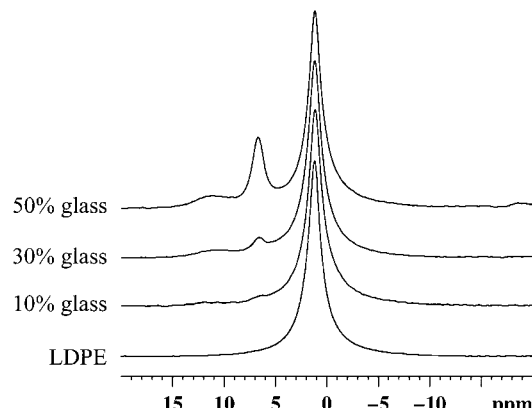


Figure 6. The ^1H MAS NMR spectra of LDPE and the TFPPE composites. In the composite materials two new resonances appear with increasing TFP glass concentration.

CPMAS resonances were observed at $\delta = -18.7$ ppm and $\delta = -6.4$ ppm. The resonance at $\delta = \sim -4.8$ ppm (fwhm ~ 300 Hz) shows a steady increase in relative concentration with decreasing TFP glass concentration, and probably represents unresolved interface species. The other three ^{31}P resonances observed have relative concentrations that are very small, or remain rather constant with variation in the hybrid composition. We cannot, at present, unambiguously identify all of the resonance peaks in the spectra. However, past work mentioned above as well as HPLC data taken for this study in the TFP glass system has shown that there are a variety of structures present in the glass other than the simple Q^1 dimers that would normally be expected to be present.^{30,32,37} This range of structures may occur as a result of the reactivity of the phosphorus atoms with the fluorine in the SnF . This phosphorus reactivity causes $\text{PO}_{(4-x)}\text{F}_x$ anions to be formed in the glass material. In addition, there are a variety of phosphate structures that can be found in hydrated glass species.^{38–40} The previously reported tendency of the TFP glass system to exhibit shear-induced crystallization under certain conditions is also expected to contribute to the complexity of the spectra.^{2,3}

^1H MAS NMR. The isotropic regions of the 1D DP ^1H MAS spectra are shown in Figure 6 for the TFPPE hybrids. Spinning of the hybrid samples at 10 kHz reduced the ^1H line width of the PE amorphous and crystalline phases ($\delta = + 1.3$ ppm) and allowed the observation of two new signals at $\delta = + 6.6$ and 10.8 ppm that appear with addition of the TFP glass (Figure 6). The changes in the relative fraction of these ^1H resonances as a function of hybrid composition are summarized in Table 3S.

^1H - ^{13}C and ^1H - ^{31}P WISE. The 2D ^1H - ^{13}C WISE NMR spectrum for the 30% TFPPE hybrid sample is shown in Figure 7. Similar 2D WISE spectra (not shown) were observed for both the 10% and 50% TFPPE hybrids. These spectra reveal a very broad ^1H resonance (cen-

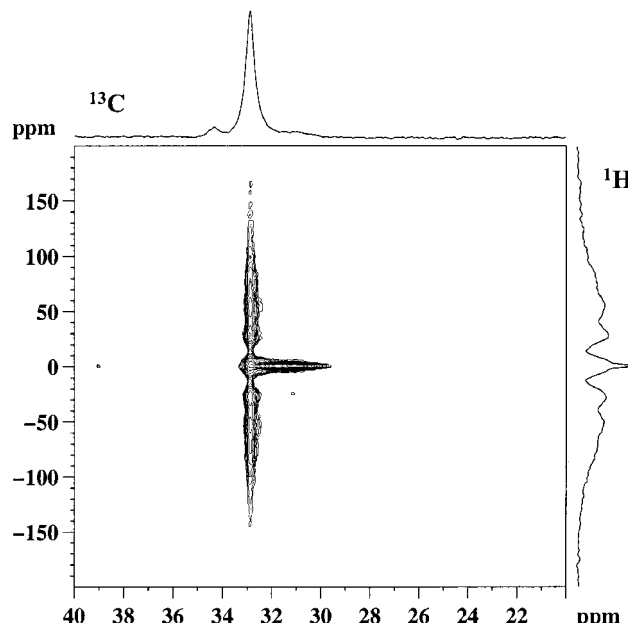


Figure 7. The 2D ^1H - ^{13}C WISE NMR spectra for the 10% TFPPE composite. The crystalline, intermediate and amorphous carbons in the PE component all correlate to the CH_2 protons at $\delta = + 1.3$ ppm.

tered at approximately $\delta = + 1.3$ ppm) for both the monoclinic and orthorhombic carbons in the PE component. The 2D WISE spectrum of the monoclinic carbon resonance ($\delta = + 34.2$ ppm) has much lower intensity relative to the orthorhombic phase and is therefore not visible at the contour levels chosen in Figure 7. The observation of a broad ^1H line width for the orthorhombic and monoclinic phases is consistent with the rigid protons of highly crystalline systems. The carbons of the amorphous PE phase ($\delta = + 31.1$ ppm), along with the carbons of the additive ($\delta = + 32.3$ ppm) are correlated to protons that have a much narrower line width. The chemical shift of this narrower ^1H resonance is still observed at $\delta = + 1.3$ ppm. This demonstrates that both the crystalline and amorphous methylene ^1H have the same chemical shift (and are combined in the relative fractions calculations in Table 3S). It should be noted that there is no correlation observed between the carbons within the amorphous PE component ($\delta = + 31.1$ ppm) and the two new ^1H resonances at $\delta = + 6.6$ and 10.8 ppm in the TFPPE hybrids. Additionally, the well resolved ^{13}C resonance at $\delta = + 38.9$ ppm of the flame retardant additive reveals a narrow ^1H line width, and shows no spatial correlation with these two new ^1H resonances. Unfortunately, the broad ^1H line width of the crystalline phase obscures the observation of any correlations between the carbons of the crystalline and intermediate PE phase and these new ^1H resonances.

The 2D ^1H - ^{31}P WISE NMR spectrum for the 50% TFPPE hybrid sample is shown in Figure 8. Similar 2D WISE spectra were observed for the 10% and 30% TFPPE hybrids. Spectral slices through the three ^1H resonances of interest are also shown. These slices show the ^{31}P spectra of the phosphorus species that are correlated with a given ^1H type. In these hybrid materials no phosphorus species are spatially correlated with the methylene protons of the PE component, since there is no apparent signal for this ^1H chemical shift, $\delta = +1.3$

(37) Otaigbe, J. U.; Tischendorf, B. C.; Sales, B. C., Unpublished HPLC data of TFP Glasses.

(38) Hartmann, P.; Vogel, J.; Schnabel, B. *J. Magn. Reson. A* **1994**, 111, 110.

(39) Wenslow, R. M.; Mueller, K. T. *J. Phys. Chem. B* **1998**, 102, 9033.

(40) Mercier, C.; Montagne, L.; Sfihi, H.; Palavit, G. *J. Non-Cryst. Solids* **1999**, 256–257, 124.

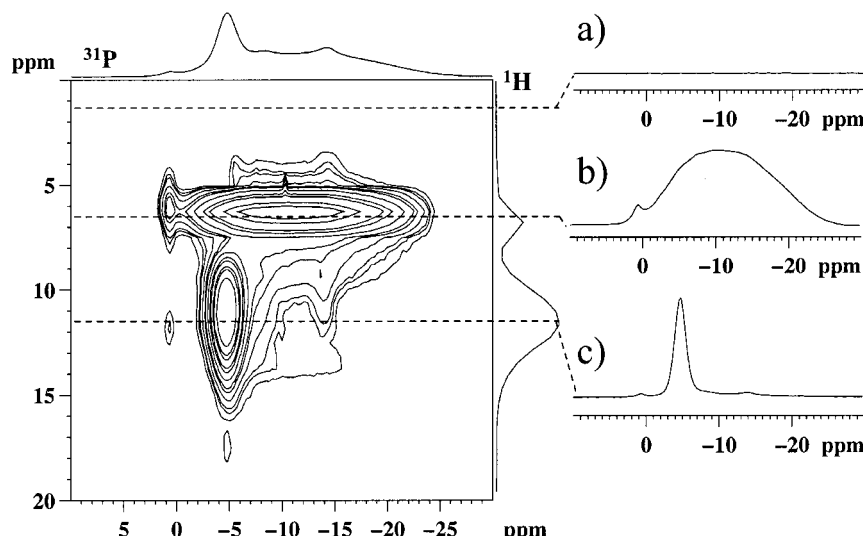


Figure 8. The 2D WISE ^1H - ^{31}P WISE NMR spectra for the 50% TFPPE composite. Spectral slices through the ^1H resonances at $\delta = +1.3$, $+6.6$ and $+10.8$ ppm are presented to the right of the 2D WISE spectra, revealing the ^{31}P species correlated with the different ^1H species.

ppm (Figure 8a). The broad ^{31}P resonance at $\delta = +11.8$ ppm is correlated exclusively with the ^1H species at $\delta = +6.6$ ppm (Figure 8b). The small ^{31}P resonance at $\delta \sim +0.7$ ppm shows correlation with both of the new ^1H species at $\delta = +6.6$ and $+10.8$ ppm. The remaining ^{31}P species ($\delta \sim -14.2$, -8.0 and -4.7 ppm) are correlated with the most downfield ^1H species at $\delta = +10.8$ ppm (Figure 8c). These results indicate that there are two types of protons associated with the glass network. If hydrolysis of the glass network has occurred because of water present in the polymer during processing, we would expect to see not only the proton resonance resulting from P–OH bonding, but also some resonance resulting from any molecular water that is left unassociated in the network. The ^1H NMR signal for unassociated water is observed between 2 and 7 ppm.³⁹ In zinc phosphate glasses, strongly absorbed surface water was found to produce a ^1H resonance at $\delta = \sim +8$ ppm.⁴⁰ In the TFPPE hybrids the ^1H resonance at $\delta = +6.6$ ppm is probably the result of absorbed water of the TFP glass surface within the hybrid, or is produced by a very weak hydrogen bonding environment. This is consistent with the correlation to the ^{31}P NMR resonances at $\delta = +0.7$ and -11.8 ppm, which are assigned to the Q^0 and Q^1 phosphate species near absorbed water, respectively. The resonance occurring at $+10.8$ ppm is indicative of a stronger hydrogen bond between the phosphate tetrahedra and the protons.³⁹ The ^1H chemical shift is consistent with intermolecular sharing of an OH or water proton between adjacent Q^1 or possibly adjacent Q^1 and Q^0 units within the TFP glass structure. The observed correlation between this hydrogen bonded proton at $\delta = +10.8$ ppm and the ^{31}P MAS NMR resonances at $\delta = -14.2$, -8.0 , -4.7 and $+0.7$ ppm results from intermolecular hydrogen bonding between a variety of different Q^1 and Q^0 phosphate species. The lack of evidence for correlation between the polymer backbone and the ^1H resonances at $\delta = +6.6$ and 10.8 (see ^1H - ^{13}C 2D WISE discussion), the weak ^1H concentration in the original TFP glass, and no corresponding ^1H NMR absorbed water signal in the original LDPE material (Figure 6) suggests that the formation of these new ^1H and ^{31}P

resonances results from the infiltration of water and subsequent hydrolysis of the TFP glass component during hybrid processing despite the care to ensure dry starting materials and the lack of steps in processing where water could have been absorbed.

DSC. The peaks of the melting endotherms for LDPE and hybrid materials were observed at 131 ± 1 °C for two consecutive runs. All samples have only a single PE melting peak, typical of LDPE. The melting temperature and calculated crystallinity for LDPE and each of the hybrids are given in Table 1S in the supporting material. The crystallinity of the 10% and 30% TFPPE hybrids are slightly higher than pure LDPE, while the 50% hybrid sample exhibited a slightly lower crystallinity. However, the accuracy of these measurements is limited in the TFPPE hybrids because of several factors including high uncertainty in the LDPE mass and low enthalpies of melting. In addition, the correlation between melting enthalpy and crystallinity may not be possible because of the presence of the intermediate components and residual strains.

Discussion

By combining these different NMR results, an improved understanding concerning the resulting structure and morphology in these TFPPE hybrids is possible. The ^{13}C NMR results show that there are no major variations in either the structure or relative phase distribution of the PE component with addition of TFP glass up to 50 vol %. A small, steady increase in the overall crystallinity is observed with higher glass loading. Both the monoclinic and orthorhombic phases are observed to increase in relative concentration with higher vol % TFP glass (Figure 4). These NMR results deviate slightly from the DSC trend that shows a decrease in the crystallinity at the highest (50%) loading. The increased crystallinity is ascribed to glass nucleation of the LDPE crystallites, thereby increasing the propensity to crystallize. The amorphous phase is reduced by $\sim 6\%$ in all three hybrid materials when compared to the pure LDPE. On the other hand, the relative fraction of the intermediate phase appears

unaffected by the addition of the TFP glass. A slight increase in the intermediate phases for the 10 vol % TFPPE hybrid is observed, but is close to the experimental uncertainty. Inspection of the ^1H - ^{13}C 2D WISE (Figure 7) demonstrates that the new ^1H species observed with increasing TFP glass concentration do not have a close proximity to the methylene protons of the amorphous PE component. Besides the increase in the overall PE crystallinity, there does not appear to be any other changes in structure that are the result of glass addition in the hybrid. The ^{31}P MAS NMR results clearly show major changes to the TFP glass component of the hybrid, including the formation of several new phosphate species that may be due to hydrolysis during the mixing process. The two new ^1H species observed in the hybrid are spatially correlated with the numerous new phosphorus species formed with increasing TFP glass loadings.

The experimental accessibility of the phase structure and dynamics of the hybrids reported here confirms our expectation of molecular-scale mixing during processing of the hybrid components in the liquid state. The low T_g and flow characteristics of the hybrid components facilitate the molecular-scale mixing as previously reported.^{1,3} The ability to combine, in a single material, inorganic (TFP) and organic (LDPE) components at the nanometer molecular length scale is thought to represent an exciting possibility with extraordinary implications for the rational design of novel multifunctional materials having a wide range of prescribed structures and properties. It is hoped that the present study will provide useful guidelines to future experimental studies and theory development for the little-studied glass-polymer hybrids.

Conclusion

These experiments demonstrate that for the TFPPE hybrids investigated there are very distinct changes in the local structure of the TFP glass component, while the PE component shows minor variations of the overall phase morphology. The ^{31}P MAS results show that there

are very pronounced differences in the TFP glass structure as a function of different volume % loadings in the hybrids. The single broad resonance characteristic of the pure TFP glass is replaced by five to six distinct new phosphorus species. There does not appear to be a ^{31}P resonance that is the same as that for the base TFP glass as Figure 5 shows. This last experimental fact indicates that there is no bulk TFP glass simply residing in the PE matrix, but instead all of the TFP glass has undergone a structural change during the formation of the hybrid.

In addition to the crystalline orthorhombic and monoclinic modifications of the PE, a number of fast relaxing, non-PE resonance structures were observed in the hybrids. These non-PE structures are ascribed to additives such as brominated flame retardant present in the as-received PE. Differences in the relaxation properties of the aforementioned structures allowed them to be reliably deconvoluted and quantified, making it possible to discern the effects of the TFP glass addition on the PE morphology in the hybrid. It is noteworthy that the percent crystallinity of the hybrid as determined by the solid-state NMR methods was found to be consistent with that obtained from differential scanning calorimetry.

Acknowledgment. Financial support of J.U.O.'s research from the U.S. National Science Foundation (DMR9733350) and the research work of his former graduate students are gratefully acknowledged. Sandia is a multiprogram laboratory operated by the Sandia Corporation, a Lockheed Martin Company, for the United States Department of Energy under Contract DE-AC04-94AL85000. Work partially performed (BCT) as a participant of the student intern program (SIP) at Sandia National Laboratories.

Supporting Information Available: Figure of the NMR pulse sequences utilized, along with three Tables detailing the ^1H , ^{13}C and ^{31}P NMR analysis and results (PDF). This material is available free of charge via the Internet at <http://pubs.acs.org>.

CM010670J